

# FUNDAMENTAL COMBUSTION AND GASIFICATION ASPECTS OF BIOMASS AND BIOMASS DERIVED GASEOUS FUELS

H.S. MUKUNDA and P.J. PAUL

Department of Aerospace Engineering, Indian Institute of Science, Bangalore-560 012

Proc. First ISMMT-ASME Joint Heat & Mass Transfer conference, Jan 1984

## Abstract

This paper considers the fundamental aspects of reactions of biomass char with air, carbon dioxide and water vapour and the flame propagation of producer gas and its components, namely carbon monoxide and hydrogen with air. The results of the conversion time of wood char spheres with the gases noted above have been presented and the role of diffusion and reaction in the controlling process are delineated. The flame propagation speeds of producer gas with mixture ratio and the flammability limits are presented. The relationship of these with those of the components, namely, CO and H<sub>2</sub> is explored. Further the propagational features of these two components with air are examined in detail. It is shown that flame structure for both these are dominated by low activation energy reactions which contribute in nearly equal proportions to the heat release. It is argued that simple minded equivalent single step reactions are poor in replicating the heat release profile. Further, it is shown that even fuels like methane, propane and other hydrocarbons (HC) have such heat release profiles with long hot tail that they cannot be modelled by single step reactions. The reasons for the peak in flame speed at fuel rich equivalence ratios are explored through the peaks of the radicals in the reactions controlling the heat release.

## Background

Over the last several decades the need for deployment of renewable energy sources for meeting energy services has been found more demanding for developing countries which have to import significant amounts of petroleum products. Amongst the several alternatives, biomass occupies a prominent role. Unfortunately, the choice of biomass as an important one is not adequately recognised. Biomass can be interpreted as stored solar energy, benign in terms of carbon sequestration and hence superior to other forms of alternate energy in terms of environment friendliness, and being capable of meeting energy demands including transportation sector.

Biomass conversion via anaerobic digestion is a slow rate process and can treat cellulose, but not lignin. The only way biomass conversion can take place completely is via combustion or better, gasification. The latter technique permits generation of combustible gas capable of being used in internal combustion engines to generate electric power.

Biomass is characterised in several ways. The more important characteristics are its density, ash content and the physical form; the melting point of ash forms another relevant feature. Materials such as wood, cotton stalk, mulberry stalk, coconut shells, and coconut frawn can be classified as woody biomass with relatively high density ( $\geq 250 \text{ kg/m}^3$ ) and low ash content ( $\leq 4\%$ ). Bagasse, sugarcane trash and leaves, rice husk, coconut coir pith, peanut shells, and other agricultural wastes

belong to what is classified as powdery biomass in recognition of the feature that the physical state of these materials and their density ( $\leq 200 \text{ kg/m}^3$ ) are such that pulverising brings all of them to almost uniform condition. Many of these materials have fairly high ash content going up to as high as 20% (as in rice husk).

Recognising the potential and the need for technologies for India, technologies related to biomass gasification and combustion for both the above classes of materials (woody and powdery biomass) have been developed at the Indian Institute of Science [1]. The technology development has gone on for the last ten years and in this process, many scientific questions have been resolved. The present paper gives an outline of some of the major questions and results and some of the yet-to-be-answered questions are brought out.

## Biomass vs. Fossil Fuels

Most of the combustion studies in the literature are focussed on fossil fuels. Of the published work in the journals of Combustion and Flame, Combustion Science and Technology, and International Symposia on combustion for the last twenty years, less than 5% of the papers pertain to biomass, whereas liquid fuels and coal take the major share of the publications. There is inadequate recognition that biomass is different from coal which has been investigated far more extensively.

Biomass is produced from the photosynthetic reaction and is constructed by nature in an orderly and well designated manner. Structurally biomass exhibits an extraordinary degree of symmetry. In contrast, coal, though is obtained from biomass and other bio-materials, has undergone very long natural processes at high pressures and temperatures, and is structurally more disordered. This feature has implications on the combustion/conversion behaviour of the chars obtained from wood/coal.

Processed liquid fuel used for combustion produces very little solid residue. Solid fuels—biomass or coal—get consumed in two stages. After ignition which is more difficult with solid fuels in comparison to liquid fuels (which is more difficult in comparison to gaseous fuels), the volatiles are first consumed. Then what remains is largely carbon in the form of porous char. This gets consumed by heterogeneous reaction with oxygen. The stoichiometric air-to-fuel ratio is typically 5.5–6.5 for biomass and from 4–10 for coal depending on the amount of ash contained in the coal. Typically, Indian coals which have 35–45% ash content have a stoichiometric fuel-air ratio of 4–5.

In biomass gasifiers, the products combustion, namely carbon dioxide and water vapour, react further with the char to be reduced to carbon monoxide and hydrogen. This process which is endothermic helps in generating combustible gas which may be used in internal combustion engines. The gas produced like this is called wood gas, coal gas or

producer gas. It is essentially thermochemical conversion of the solid fuel with substoichiometric amount of air to produce a gaseous mixture having a composition approximately of 18-20 % CO + 18-20 % H<sub>2</sub> + 3-4 % CH<sub>4</sub> + 10-12 % CO<sub>2</sub> + rest N<sub>2</sub> for wood. The two interesting scientific problems are the prediction of the gaseous composition from the complex oxidation-reduction reactions and the combustion properties of the producer gas.

Predicting the outlet gas composition amounts to modelling the reactor operation and such a modelling will call for a precise understanding of the reduction reaction between char and carbon dioxide and water vapour. This is one subject discussed here in some detail. The combustible properties of the producer gas of interest are its stoichiometry, flame temperature, and flame propagation characteristics. While the first two aspects are elementary, the last item provides interesting features since the gas is composed of two gases: carbon monoxide which has a low flame speed of 0.2 m/s at stoichiometry and a peak of 0.4 m/s at  $\phi = 1.4$ , and hydrogen which has a very high flame speed of 2.2 m/s at stoichiometry and a peak of 3.8 m/s at  $\phi = 1.4$ . The interesting question is what the flame speed of the mixture having equal amounts of CO and H<sub>2</sub> would be. Would it simply be a mean or does CO or H<sub>2</sub> exert greater influence on the flame propagation behaviour. This is the second subject of examination here:

## Wood Char Reaction Behaviour

Wood char reacts with air to form carbon dioxide; it also reacts with (a) carbon dioxide to produce carbon monoxide and (b) water vapour to produce carbon monoxide and hydrogen. These occur at widely differing rates because reaction with air is exothermic and those with carbon dioxide and water vapour are endothermic. The latter two reactions have high activation energy and are strongly temperature dependant. While conversion of char in air at ambient conditions or oxygen rich conditions is known to be diffusion limited, kinetics is important for the reduction reactions with CO<sub>2</sub> and H<sub>2</sub>O. Wood charcoal, known for its high reactivity, has been studied much less than coal char for the evaluation of either the kinetic parameters or conversion times in well defined geometries. Most of the earlier work on char gasification has been done on the coal char and on small particles in the range of .02-1.5 mm diameter. The experimental studies [2,3,4,5,6] are directed towards a packed bed gasification, with very limited work on single particles [7,8,9] Blackwood and Ingeme [10] have conducted studies on coconut char in the form of packed bed of powder. The reduced particle size in the above studies is aimed at eliminating the diffusional control. By reducing the particle size to below a certain level it is assumed that the conversion process is reaction controlled; only in a few cases is there an independent experimental confirmation of this feature. Apart from this, there are two studies where experiments have considered larger sizes which imply inclusion of diffusional aspects. Groeneveld [7] has performed experiments on a plane one-dimensional configuration of wood char in a quiescent environment of carbon dioxide-nitrogen mixture. These results are interpreted along with a theory which makes the isothermal approximation. The rate expression used is derived assuming equal rates of reaction of carbon dioxide and water vapour with char, which is inconsistent with the earlier experimental data on coal char [4]. The other study is by Standish and Tanjung [9] who have reported the results of reaction of Australian rubber wood char spheres of 10-20 mm diameter with carbon dioxide-nitrogen mixtures at temperatures between 1150-1450 K as a function of flow rates of the gaseous mixture. This work has very interesting experimental results. Dasappa *et al* [11] have repeated part of the experiments and a theoretical model was set up which accounts for heterogeneous reaction and diffusion into pores along with the effects of free and forced convection. This work has since been modified to account for the effects of ambient oxygen and water vapour. To validate the computational code, experiments on the effects of oxygen on the burn time of the char spheres as well as conversion time with water vapour at temperatures of 900-1000 K have been obtained. The

data on oxygen includes the cases of extinction at low levels of oxygen concentration; the data on water vapour are new.

The experimental set up is described in detail in Dasappa *et al* [11]. The sample of 3-15 mm diameter is suspended from a balance inside the reactor (of 40 mm diameter) maintained at the required temperature and the reactant gas is passed through the reactor. The variation of mass of the sample with time, the total conversion time, and the mass flow rate of the gas are recorded. Char samples were prepared in two different ways: by burning dried wood spheres in air and quenching it at the end of flaming combustion or by slow heating of wood spheres in the absence of oxygen. In some cases, the char samples were finished to obtain spherical geometry. The density of char obtained by fast pyrolysis was  $180 \pm 20$  kg/m<sup>3</sup> and that obtained by slow pyrolysis was  $400 \pm 30$  kg/m<sup>3</sup>. During the experiments in air or vitiated air, the weight loss was accompanied by enveloping of char by ash layer and the glowing char was visible through the ash layer. In the case of experiments with reduced oxygen mass fraction, the time of extinction could be identified by the disappearance of the glow. In the experiments with carbon dioxide and water vapour, it was observed that the char sphere was nearly of the same size till about 50-70 % burn time when the ash layer covering the sphere was noticed. However, the carbon core was visible through the ash layer till the end of the burn time. Other aspects of the experiments can be found in Sridhar *et al* [12] and Dasappa *et al* [11].

A mathematical model has been set up for the processes during the combustion or gasification of porous carbon spheres including diffusion and convection of the species and energy in the porous medium, and heterogeneous reaction between the gaseous species and the char. These are modelled in the present analysis using the unsteady spherically symmetric one-dimensional conservation equations [8,11,12]. In the present model the mechanism of overlap and intersection of growing pores is neglected. More sophisticated model is not used because the change in conversion is not significant with pore surface change for wood char of high initial porosity. This feature is more relevant to wood char where the initial porosity is very large ( $\sim 0.8$ , [11] compared with the coal char which has generally low porosity ( $\sim 0.2$  [3]). Wood which has much higher fraction of volatiles ( $\sim 75-80$  % compared to 30-50 % in coals) leaves a char of relatively lower density and higher porosity. The model uses the thermodynamic and transport property data from other sources [11]. The model for the heterogeneous reaction and the kinetic parameters including the activation energy are obtained from Blackwood and Ingeme [10]. Only one free parameter namely the frequency factor in the expression is set by comparing with the experimental data on the conversion time at one condition. There are no other free parameters in the theory.

The most important results of the experiments and theory are set out in Fig. 1. This figure shows the data of burn time normalised by char density with diameter. The normalisation by density is to account for variations in the char density and is consistent with the expectations of theory—diffusion limited or reaction limited. For the purposes of clarity the only results for pure CO<sub>2</sub> and H<sub>2</sub>O at 1273 K are shown. There are several important features in the figure. The conversion rate with air can be summarised by  $t_b/\rho_c \approx A d_0^n$  where  $t_b$  is the burn time in s,  $\rho_c$  is the char density in g/cm<sup>3</sup> and  $d_0$  is the diameter of the char sphere in mm. The values of  $A$  and  $n$  are 21.5 and 1.85 for data at 300 K ambient, and 11.0 and 2.0 for data at 1000 K. The exponent 1.85 at 300 K departs from 2 due to buoyancy effects; the values of  $n$  are indicative of diffusion limitedness of the conversion process—in this case, combustion. Conversion with carbon dioxide leads to  $t_c/\rho_c \sim 300.0 d_0^{0.5} \exp[-35300(1/T - 1/1273)]$ , where  $t_c$  is the conversion time in s and the exponent on  $d_0$  is indicative of nearly equal contributions by diffusion and reaction. The large value for the activation temperature is typical of these reactions. Conversion with water vapour leads to  $t_c/\rho_c \sim 43.6 d_0^{1.41}$  (at 1273 K). The exponent 1.4 on  $d_0$  is indicative of greater influence of diffusion. From the Figure it is also clear that water vapour is far more reactive compared to CO<sub>2</sub>. These results also suggest that the choice of sphere and these simple experiments lead to direct indication of

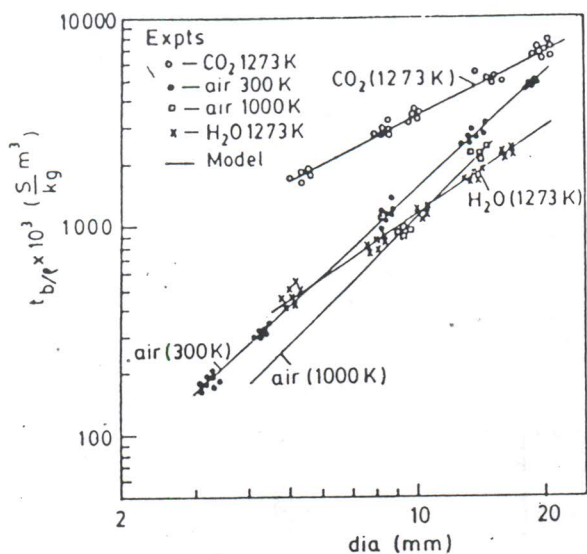


Figure 1: Plot of  $t_b/\rho$  for char-air system and  $t_c/\rho$  for char-carbon dioxide and water vapour systems with char diameter.

reactivity of the system. The good match between the experiments and theory for both air and  $\text{CO}_2$  cases is evident. The theoretical curves have been extended to very low diameters of the char sphere. From these it can be noted that the conversion time is nearly independent of diameter. It is in this limit diffusion is so fast and reaction so slow that the center of the sphere is no different from the surface and reaction occurs uniformly in the sphere. This implies that the conversion process will be independent of the diameter. Typically, the value of this for wood char at 1273 K is 100  $\mu\text{m}$ . For lower temperatures, the limiting size below which the process is reaction limited will be larger. Also, for coal chars which are known to be less reactive compared to wood char the limiting size could be larger. A clear way of expressing the limiting condition is to plot the ratio of the rates and the temperature at the center and the surface with diameter. Such a plot is seen in Fig. 2. It appears that unless the deviation of the temperature ratio falls below a few degrees the process tends to depart from rate limited condition.

The results for combustion with  $\text{O}_2\text{-N}_2$  mixtures with reduced oxygen fractions are shown in Fig. 3. The conversion is complete for oxygen mass fraction exceeding that in air; below this value, the degree of conversion depends sharply on the fraction of oxygen. Below 14%  $\text{O}_2$ , the conversion process is totally inhibited. These results are consistent with the earlier results by Rashbash and Langford [13] and Watson

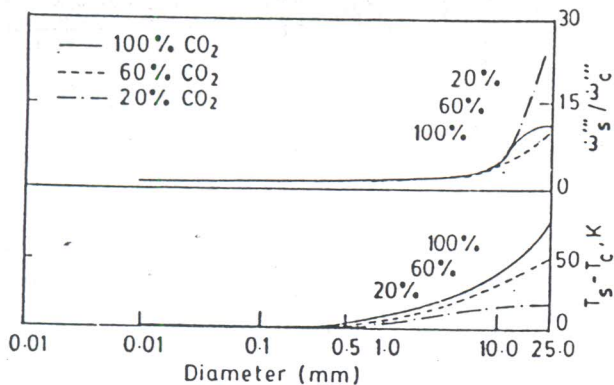


Figure 2: Plot of the core to surface temperature and reaction rate ratios with char diameter.

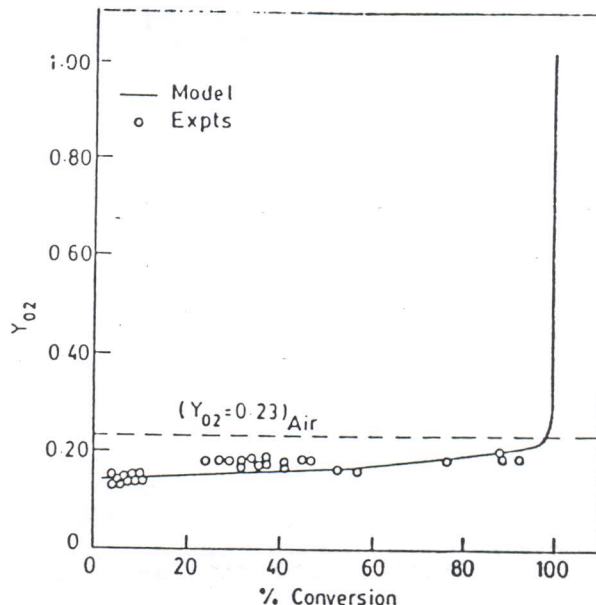


Figure 3: Plot of oxygen mass fraction with percentage conversion for char-diluted air system.

*et al* [14], where combustion of wood and paper were considered respectively. From the analysis for  $Y_{\text{O}_2} = 0.14$ , the causes for extinction were uncovered; the heat generation at the surface during the initial stage is very low and heat losses dominated so that reaction could not pick up.

The results indicated above form a part of the model for predicting the composition of a wood gasifier, a feature known to be rate limited. While there have been such models for coal gasifiers [15] these models are so complex and contain several assumed reactions that they are not well founded in terms of robustness of their component features. The subsidiary components are not adequately tested. It is hoped that the use of the presently indicated models will provide a more sound basis for predicting gasifier outlet composition. This is the line of current study.

## Flame Propagation in Producer Gas-Air Mixture

### The Issues

Producer gas composition from wood gasifiers are typically as follows:  $\text{CO} = 20 \pm 2\%$ ,  $\text{H}_2 = 20 \pm 2\%$ ,  $\text{CH}_4 = 3 \pm 1\%$ ,  $\text{CO}_2 = 10 \pm 2\%$  and  $\text{N}_2 = \text{Rest}$ . In a typical downdraft wood gasifier of the kind developed at the Indian Institute of Science, the presence of tar, constituting higher hydrocarbons (HC), is limited to less than 50 ppm to enable the use of the gas in reciprocating engines for power generation.

The striking feature of the composition is the near equal fraction of  $\text{CO}$  and  $\text{H}_2$  in relatively large fractions. These two gases are characterised by the extremes in reactivity— $\text{CO}$  being low (can be taken to be comparable to or slightly lower than  $\text{CH}_4$ ) and  $\text{H}_2$  being very high. The peak flame speed of  $\text{CO}$ -air mixture is 40 cm/s at  $\phi = 1.4$  and of  $\text{H}_2$ -air mixture is 300 cm/s at  $\phi = 1.7$ . A common feature of the two mixtures is the fact that peaks do not occur near  $\phi = 1$ .  $\text{H}_2$ -air mixtures are known to have low activation energy [16,17].  $\text{CO}$ -air mixtures have been investigated by several leading researchers [18,19,20] and the data [19] indicates to reasonably high activation energy and the analysis [20] indicates to low activation energy. The picture is still unclear. These aspects need to be clarified. A further reason to pursue the study of producer gas-air mixture is that it is useful to understand what the flame speed of the mixture of gases having widely different flame speeds would be. Also there has been no earlier work on the experimental data

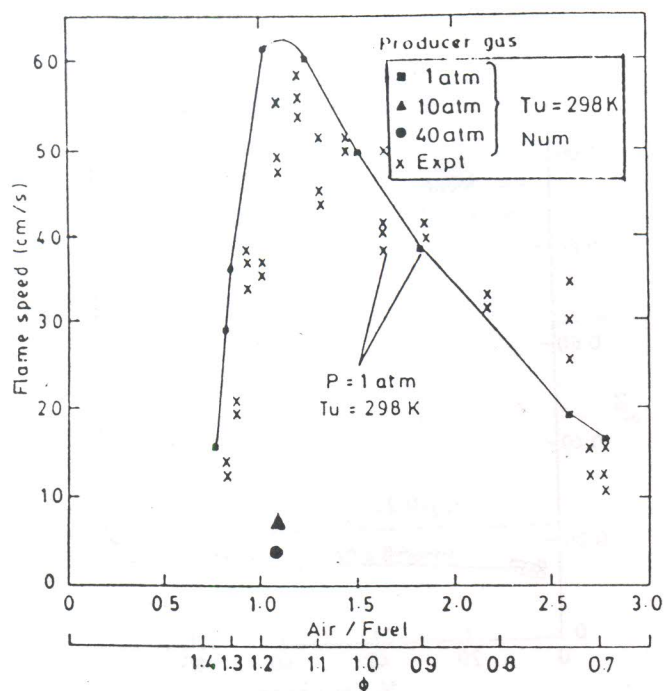


Figure 4: Plot of the flame speed vs air-to-fuel ratio and equivalence ratio for producer gas (experiments and calculations).

on the flame speed of producer gas-air mixtures.

#### Flame Structure of Producer Gas-Air Mixture

Motivated as above, work has been carried out at IISc to experimentally determine the flame speeds and the flammability limits of producer gas-air mixtures [21] and also to explore the structure of these flames [22,23]. An approach to understanding the structure of these flames was derived from a similar study of  $\text{CH}_4$ -air flames earlier [24]. What is being set out below is a comprehensive view point derived from these studies.

Figure 4 shows the experimentally measured flame speeds [21] as a function of air-to-fuel ratio (also  $\phi$ ) at ambient pressure. The figure also shows the computed flame speeds at ambient pressure and at two higher pressures [23]. The spread in the data due to some variations in the composition of the gas is not unexpected during a normal gasifier run due to variations in the size, moisture content of wood chips and the temperature build up inside the gasifier. The gas composition was measured several times during the run. These were found to be within the limits indicated. The calculations were made with a composition: 23% CO, 22%  $\text{H}_2$ , 2%  $\text{CH}_4$ , 12%  $\text{CO}_2$ , and rest  $\text{N}_2$  since it is at one end of variation of CO and  $\text{H}_2$ . The calculations were made with kinetic data of C-H-O system used in earlier studies from the laboratory [25].

The figure has several interesting results. The peak flame speed is around  $55 \pm 5$  cm/s and occurs at air-to-fuel ratio of 1.2 and  $\phi$  of 1.15. The limits of propagation occur at  $\phi = 1.35$  (rich) and 2.7 (lean). The predictions envelope the data on the rich and some portions of the lean side. The peak flame speed is 60 cm/s and occurs at  $\phi \approx 1.15$ . In several aspects the predictions match with the experimental data quite well. An interesting feature of the result is that the flame speed drops to 5 cm/s at a pressure of 10 atm and 3 cm/s at 40 atm. These flame speeds computed for adiabatic conditions are so low that under the influence of the normal heat loss, the flames will not propagate at these pressures.

Figure 5 shows the plot of flame speeds of CO-air and  $\text{H}_2$ -air as a function of the equivalence ratio. Though for CO and  $\text{H}_2$ -air systems the peak flame speeds occur at  $\phi = 1.45$  and 1.7 respectively, the peak flame speed for producer gas occurs at  $\phi = 1.15$ . To understand this

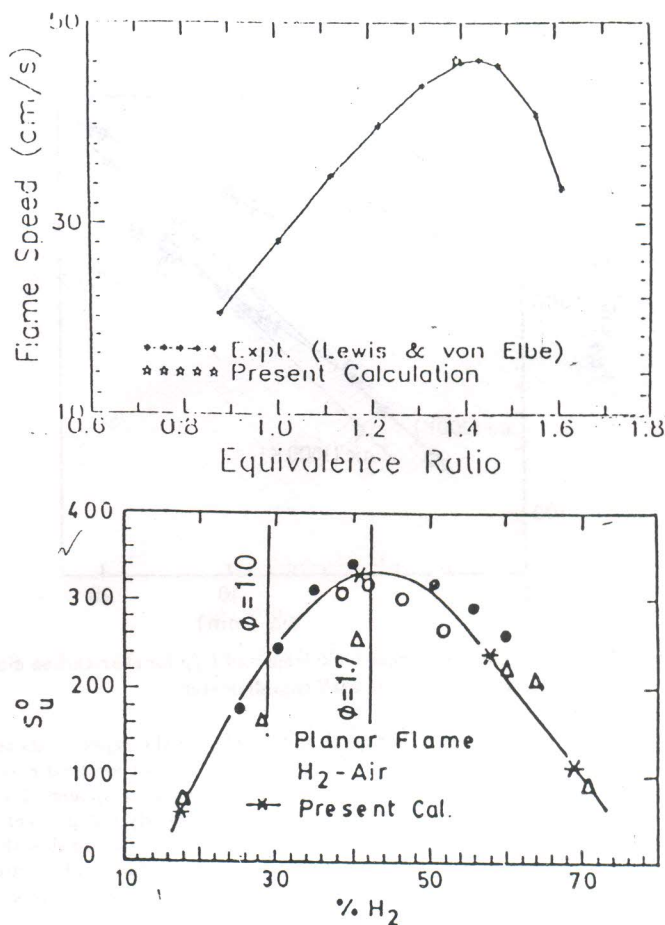


Figure 5: Plot of Flame speed vs air to fuel ratio for  $\text{H}_2$ -air and CO-air mixtures.

behaviour computations were made with 41.5%  $\text{H}_2$ , 12.5%  $\text{CO}_2$ , Rest  $\text{N}_2$  and 41.5% CO, 1%  $\text{H}_2\text{O}$ , 11.5%  $\text{CO}_2$ , and Rest  $\text{N}_2$ . These compositions are derived by taking only one major reactant while the inert component held the same. The flame speeds for these compositions are 98 cm/s and 9.8 cm/s at  $\phi = 1$ . The average flame speed of these two mixtures matches with that of producer gas. However, it cannot be expected to match for all other mixture ratios because of the anomalous behaviour in the value of equivalence ratio at which the flame speed peaks.

It was thought worthwhile examining the heat release profile for the three cases considered. This thinking has background that needs to be explained. In view of the possibility of analytical solutions, in fluid flow problems including that of flame propagation, single step reactions have been extensively treated in the literature, largely based on asymptotic techniques. One important issue concerning the choice of an equivalent single step reaction is the question as to how well the heat release rate profile with temperature is replicated. While an adiabatic reactor calculation leads to this result in a direct sense, the variation will be affected by diffusional factors in adiabatic propagating flames. If we treat only an adiabatic flame a good replication of the heat release rate profile has the implication that the overall flame properties are well predicted. This view point seems to have been tacitly assumed but not explicitly asserted. The number of studies which use this method of plotting are not many [26,24], but seems to be becoming more recognized in recent times [27]. The importance of the plot can be recognised if we note that the heat release rate ( $H_r$ ) of the equivalent single step reaction for a

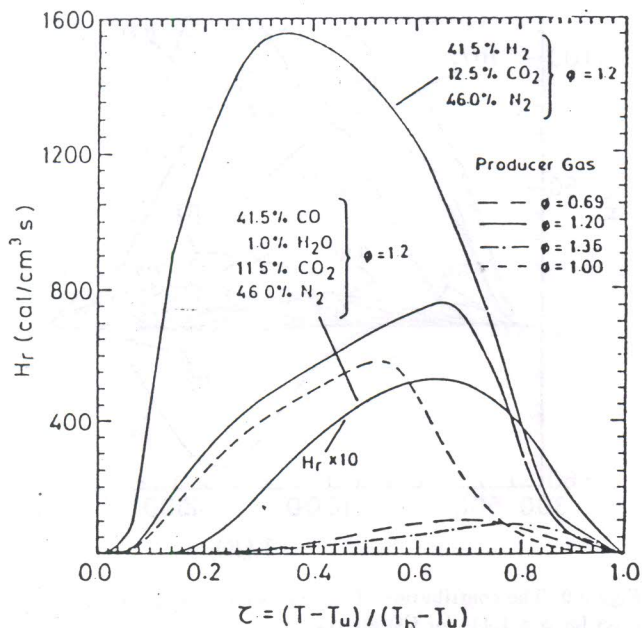


Figure 6: The heat release rates vs  $\tau = (T - T_u)/(T_{ad} - T_u)$  for producer gas,  $H_2$ - $CO_2$ - $N_2$ -air ( $\phi = 1.2$ ) and  $CO$ - $CO_2$ - $N_2$ -( $H_2O$ )-air ( $\phi = 1.2$ ) compositions.

second order reaction can be expressed by

$$H_r = A(1 - \tau)\left(\frac{1}{\phi} - \tau\right)\exp\left(-\frac{E}{RT}\right) \quad (1)$$

where  $\tau = (T - T_u)/(T_{ad} - T_u)$  with  $T_{ad}$  and  $T_u$  being the adiabatic and initial temperatures,  $\phi$  is the equivalence ratio,  $R$  is the universal gas constant and  $E$  the activation energy, and  $A$  a dimensional constant. The above equation is taken valid for lean mixtures. For rich mixtures one needs to replace  $1/\phi$  by  $\phi$ . From a knowledge of the temperature at which  $H_r$  is a maximum (from the full chemistry calculation), the activation energy can be obtained as

$$E = \frac{(1 + \frac{1}{\phi} - 2\tau_m) RT_m^2}{(\frac{1}{\phi} - \tau_m)(1 - \tau_m)(T_{ad} - T_u)} \quad (2)$$

Where  $\tau_m$  is the  $\tau$  at maximum  $H_r$ . Again, the results for lean and rich mixtures should be obtained as indicated above. Having obtained the activation energy, one can compute the activation parameter,  $\beta = E/RT_{ad}$  used extensively in asymptotic analyses of flame structure. In these analyses, it is usually assumed that  $\beta \rightarrow \infty$ . Typical values quoted to be large are 10-15 [28] and tests for accuracy of asymptotic results for flame speeds have been shown to be satisfactory for  $\beta$  upwards of 10 [29]. For large  $\beta$ ,  $\tau_m$  is close to unity. If  $\tau_m$  is much less than unity, the activation parameter will not be high.

A plot of the heat release profile with  $\tau$  is shown in Fig. 6 for selected compositions. It can be seen that for both 41.5%  $H_2$  + 12.5%  $CO_2$  + 46%  $N_2$  and 41.5%  $CO$  + 11.5%  $CO_2$  + 1.0%  $H_2$  + 46%  $N_2$  compositions the peak heat release rates are widely different as 1550 and 525  $cal/cm^3 s$  with peaks at  $\tau = 0.3$  and 0.5 respectively. Both these are so low (the estimated  $\beta$  for the two cases are 0.7 and 3.6 respectively) that it is safe to infer that the details of chemistry matter considerably. The fact that peak in heat release rate for producer gas occurs at  $\tau = 0.7$  and the hunch back nature of the heat release profile imply that strong diffusional effects are altering the composition in the flame, a feature related to  $H_2$ . The coupling between the two reaction sets ( $CO$  and  $H_2$ ) is strong as will be noted from subsequent results on  $H_2$ -air and  $CO$ -air flames. Thus one might infer the behaviour seen in producer gas as being due to the

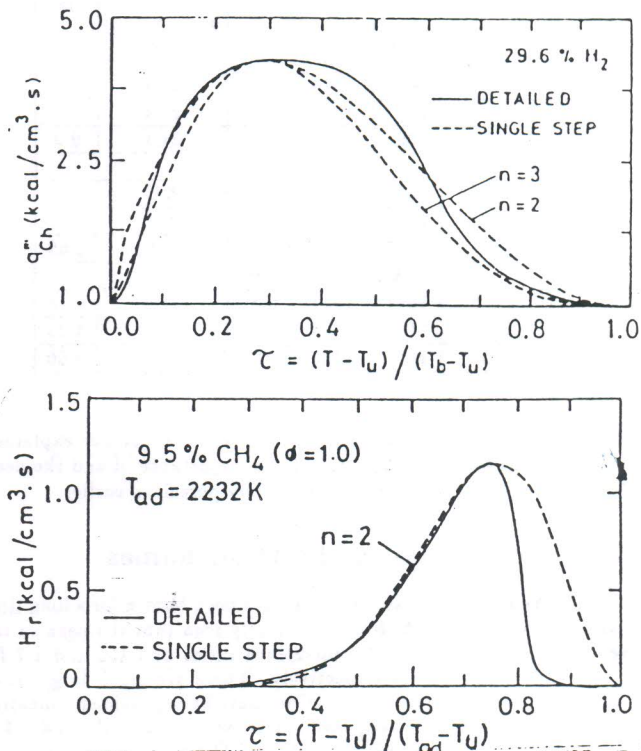


Figure 7: The heat release rates vs  $\tau = (T - T_u)/(T_{ad} - T_u)$  for stoichiometric  $H_2$ -air,  $CH_4$ -air mixtures.

high heat release of  $H_2$ -air system and the non-normal diffusion coupled to the slowly reacting and heat releasing  $CO$ -air system.

### The Importance of Chemistry

While the results noted above refer to producer gas, it is useful to inquire if there is a greater degree of generality in the statements of need for full chemistry in understanding flame behaviour. For this purpose,  $H_2$ -air,  $CO$ -air and  $CH_4$ -air systems are chosen. Plots of the heat release rates with full chemistry and equivalent single step chemistry for stoichiometric  $H_2$ -air and  $CH_4$ -air [24] are presented in Fig. 7. There are some interesting features in the plots. The temperature at peak heat release rate, and hence  $\tau_m$ , is low for  $H_2$ -air (this is also true for  $CO$ -air flame as will seen later). The more dramatic feature of  $CH_4$ -air flame ( $\phi = 1$ ) is that the heat release profile for full chemistry falls sharply at  $\tau = 0.8$ . The implication is that the temperature approaches the adiabatic value rather slowly since the driving force in heat release is not high. This feature is apparently not limited to  $CH_4$  alone. Almost all HC's seem to possess it. For instance, measurements of the temperature profile by Law *et al* [30] for  $C_2H_6$  show this feature. Propane-air system also has the same long hot tail. It appears to be the characteristic of HC chemistry. Thus while one can get parameters for equivalent single step chemistry, the replication of the heat release profile for stoichiometric and near stoichiometric HC-air mixtures through single step chemistry is virtually impossible. The values of various aspects of heat release profile are summarised in Table 1 for these and other compositions. It can be seen that even for stoichiometric  $CH_4$  and  $C_3H_8$  air mixtures, the value of  $\beta < 7$ . It is only for lean  $CH_4$ -air mixtures that one gets  $\beta$  much larger than 10. Thus the strict applicability of asymptotic analyses is really limited to lean HC mixtures, since, (1) the heat release profiles of near stoichiometric HC flames cannot be well replicated by single step chemistry and the value of  $\beta$  is not large enough, (2) the very rich mixtures are complicated by their sooting features, (3)  $H_2$ -air systems have such low activation energy that chemical details cannot be ignored, and

Table 1: The estimated values of  $E$  and  $\beta$  for the fuel-air mixtures considered

Sl. Nos	Eq. ratio $\phi$	$T_{ad}$ K	$T_m$ K	$r_m$	$E$ (kcal/mol)	$\beta$
CH <sub>4</sub> -air flames						
1	0.6	1668	1518	0.89	31.4	10.4
2	1.0	2232	1774	0.76	27.4	6.2
3	1.5	1867	1742	0.92	34.1	9.2
H <sub>2</sub> -air flames						
4	0.513	1670	1112.2	0.60	6.0	1.8
5	1.65	2187	902.5	0.32	4.2	0.97
6	3.27	1757	881.6	0.4	9.4	2.69
C <sub>3</sub> H <sub>8</sub> -air flames						
7	0.775	1881	1564	0.80	21.6	5.78
8	1.0	2164	1604	0.70	18.3	4.25
9	1.5	1857	1436	0.73	31.7	8.00

(4) CO-air systems have a similar problem which is further explained below. This calls for the recognition of the importance of and the need for full chemistry in a manner not adequately perceived earlier.

### Behaviour of H<sub>2</sub>-air and CO-air flames

The flame speeds of these two mixtures have been known for a long time and are presented in Fig. 5. It can be clearly seen that the peak in the flame speed occurs at fuel rich equivalence ratios of 1.459 and 1.7 for CO-air and H<sub>2</sub>-air mixtures respectively. These are much larger than for typical HC-air mixtures. Explanations have been provided indicating that for H<sub>2</sub>-air system the large diffusional velocities of H<sub>2</sub> and a few other components are responsible and for CO-air system chemistry is responsible [20]. Apart from general statements, no detailed exploration of this interesting feature seems available.

In seeking an explanation, it was hypothesized that the effects must be related to the heat release rate profiles and therefore, several com-

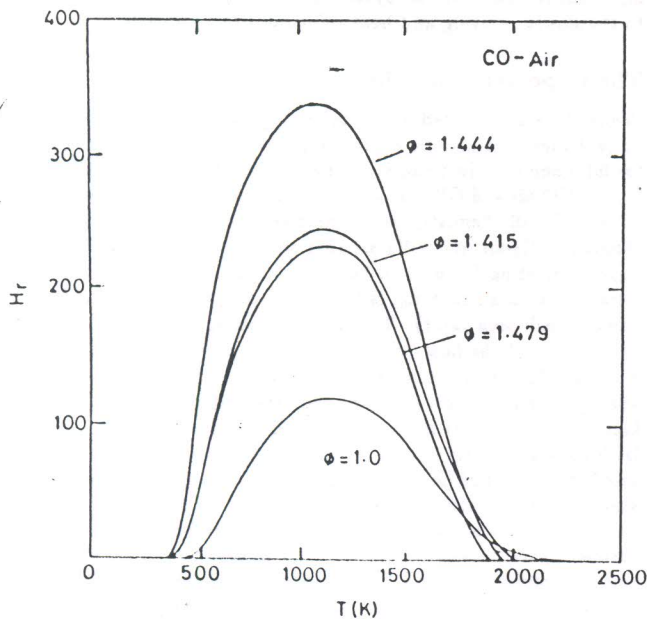


Figure 8: Heat release rates vs Temperature for  $\phi = 1.0, 1.415, 1.444, 1.48$  for CO-air.

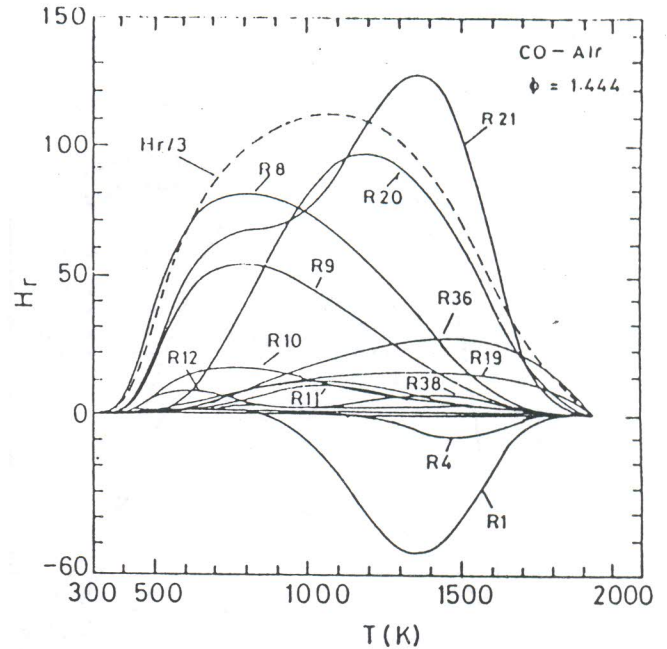


Figure 9: The contribution of various reaction steps to the heat release rates for  $\phi = 1.444$  for CO-air system

positions around the peak flame speed mixture ratio were chosen and calculations of the flame speed and structure were made. The contribution to the heat release rate from individual reactions were assessed. Figure 8 contains the plots of heat release rates with temperature at various  $\phi$ . It can be seen that the heat release rates are substantially higher at  $\phi = 1.444$  in comparison to other cases. To examine the causes further, the contributions from individual reactions for  $\phi = 1.0, 1.415, 1.459, 1.48$  were obtained. Those for  $\phi = 1.444$  are shown in Fig. 9 (others behave in an identical manner albeit the magnitude). The reaction numbers in the figure are the same as shown in Table 2. The temperature at which the overall heat release rate peaks is lower than the temperatures at which most individual reaction rates peak. The heat release

Table 2: The kinetic data on some of steps in the CO/air Reaction Scheme of Warnatz [31],  $E$  in kcal/mole,  $A_f$  in  $\text{cm}^3, \text{s}$  units.

No.	Reaction	$A_f$	$m$	$E$
R1	$\text{OH} + \text{O} = \text{O}_2 + \text{H}$	$1.8 \times 10^{13}$	0.0	0.0
R2	$\text{O} + \text{H}_2 = \text{OH} + \text{H}$	$1.5 \times 10^7$	2.0	31.6
R3	$\text{OH} + \text{H}_2 = \text{H}_2\text{O} + \text{H}$	$1.0 \times 10^8$	1.6	13.8
R4	$\text{OH} + \text{OH} = \text{H}_2\text{O} + \text{O}$	$1.5 \times 10^9$	1.14	0.0
R5	$\text{H} + \text{H} + \text{M}' = \text{H}_2 + \text{M}'$	$9.7 \times 10^{16}$	-0.6	0.0
R6	$\text{H} + \text{OH} + \text{M}' = \text{H}_2\text{O} + \text{M}'$	$2.15 \times 10^{22}$	-2.0	0.0
R8	$\text{H} + \text{O}_2 + \text{M}' = \text{HO}_2 + \text{M}'$	$2.0 \times 10^{18}$	0.8	0.0
R9	$\text{H} + \text{HO}_2 = \text{OH} + \text{OH}$	$1.5 \times 10^{14}$	0.0	4.2
R10	$\text{H} + \text{HO}_2 = \text{H}_2 + \text{O}_2$	$2.5 \times 10^{13}$	0.0	2.9
R11	$\text{O} + \text{HO}_2 = \text{OH} + \text{O}_2$	$2.0 \times 10^{13}$	0.0	0.0
R12	$\text{OH} + \text{HO}_2 = \text{H}_2\text{O} + \text{O}_2$	$2.0 \times 10^{13}$	0.0	0.0
R14	$\text{OH} + \text{OH} + \text{M}' = \text{H}_2\text{O}_2 + \text{M}'$	$3.25 \times 10^{22}$	-2.0	0.0
R19	$\text{CO} + \text{H} + \text{M}' = \text{CHO} + \text{M}'$	$6.9 \times 10^{14}$	0.0	7.0
R20	$\text{CO} + \text{O} + \text{M}' = \text{CO}_2 + \text{M}'$	$7.07 \times 10^{13}$	0.0	19.0
R21	$\text{CO} + \text{OH} = \text{CO}_2 + \text{H}$	$4.4 \times 10^6$	1.5	-3.1
R36	$\text{CHO} + \text{H} = \text{CO} + \text{H}_2$	$2.0 \times 10^{14}$	0.0	0.0
R38	$\text{CHO} + \text{O} = \text{CO}_2 + \text{H}$	$3.0 \times 10^{13}$	0.0	0.0

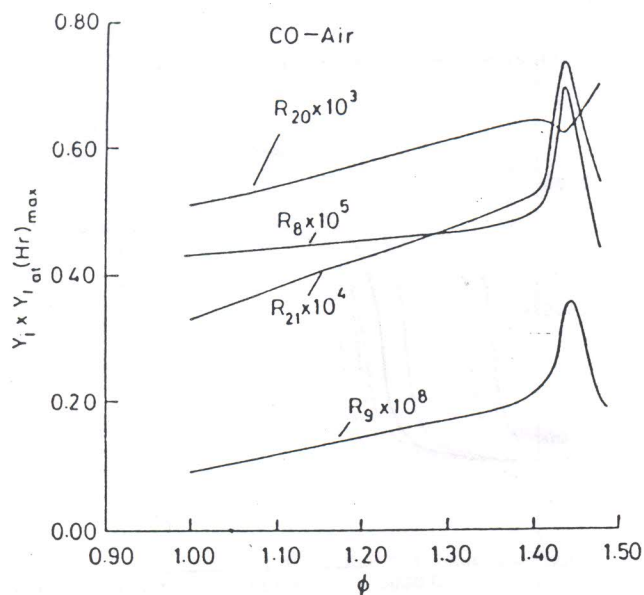


Figure 10: Plot of the product of reactant mass fractions at peak heat release rate with equivalence ratio for CO-air and H<sub>2</sub>-air systems.

rate of some reactions are partly nullified by others such that the overall peak heat release occurs at a lower temperature. The contribution to heat release to come from more than one reaction. The four reactions which make the most contributions are,  $\text{CO} + \text{OH} \leftrightarrow \text{CO}_2 + \text{OH}$ ,  $\text{CO} + \text{O} + \text{M}_1 \leftrightarrow \text{CO}_2 + \text{M}_1$ ,  $\text{H} + \text{HO}_2 \leftrightarrow \text{OH} + \text{OH}$ ,  $\text{H} + \text{O}_2 + \text{M}_1 \leftrightarrow \text{HO}_2 + \text{M}_1$ . The radicals which matter are OH, HO<sub>2</sub>, H and O. Some of the reactions were identified as important earlier also [18,19,20], but the relative importances of these reactions had not been identified, partly because these studies had different aims. In order to seek the causes for the peak in flame speed at fuel rich condition, the dependence of these reactions on temperature and mass fractions of the participating species was sought. The four reactions considered have either zero or low activation energies as can be noted from Table 2. The influence of temperature which is a function of equivalence ratio is small. The plot of the product of mass fractions of the reactants at peak heat release rate as a function of equivalence ratio shown in Fig. 10 indicates the peak in the product of mass fractions at  $\phi = 1.459$  and sharp drop on either side except in the case of one reaction namely,  $\text{CO} + \text{O} + \text{M}_1 \leftrightarrow \text{CO}_2 + \text{M}_1$ . The dip in this case is the smallest for  $\phi = 1.459$ . Thus this composition is the most reactive, weak and since the overall peak in heat release rate is caused by several reactions, this weak dip does not matter. Thus the peak in flame speed with equivalence ratio is caused by the peak in the product of mass fractions of the radicals. The contribution to peak heat release is so equally divided between these reactions that it is not possible to isolate the species or reactions better than delineated now. It is further possible to establish whether diffusional factors have played any major role in causing the peak at fuel rich conditions. A plot of temperature with time from the calculation of an adiabatic reactor for different compositions identified above at the same starting temperature of 900 K as shown in Fig. 11 indicates that the time taken to reach say 90% adiabatic temperature and therefore, propagates the fastest.

The results for H<sub>2</sub>-air are similar. Calculations for  $\phi = 1.0, 1.459, 1.7$ , and  $2.02$  for H<sub>2</sub>-air have been made. Fig. 12 shows the overall heat release rate for several values of  $\phi$ . Here the peak in heat release rate occurs at  $\phi = 1.7$ . The contributions of various reaction steps is presented in Fig. 13. The three important heat releasing reactions are  $\text{OH} + \text{H}_2 \leftrightarrow \text{H}_2\text{O} + \text{H}$ ,  $\text{H} + \text{O}_2 + \text{M}_1 \leftrightarrow \text{HO}_2 + \text{M}_1$ ,  $\text{H} + \text{HO}_2 \leftrightarrow \text{OH} + \text{OH}$ . Of these, the latter two reactions are the same as for CO-air system. The importance of the reactions does not change with stoichiometry similar to CO-air system. The contribution from the three reactions is

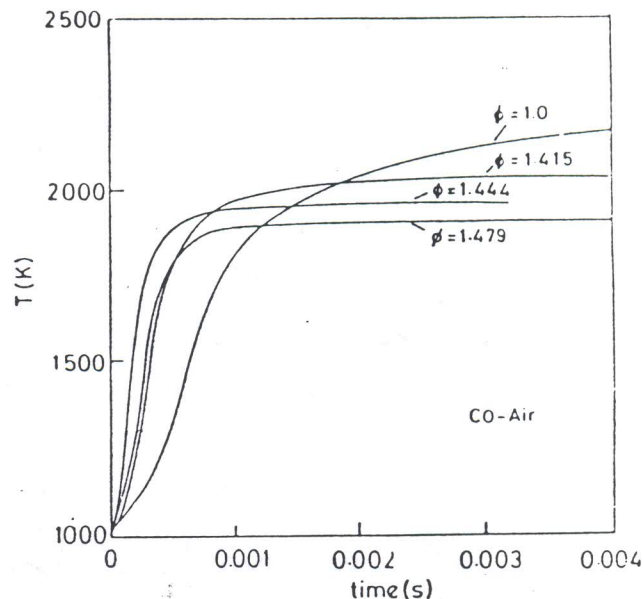


Figure 11: Plot of temperature vs time for an adiabatic reactor (CO-air).

of significant magnitude as in the case of CO-air and the peak is broad. The activation energies of these steps is small and the plot of the product of mass fractions of the reactants as shown in Fig. 14 indicates to peak at  $\phi = 1.7$ . Even though for the first reaction noted above the peak does not occur at  $\phi = 1.7$ , its contribution is not the largest. Thus ( $\text{Y}_\text{H}\text{Y}_{\text{O}_2}$ ) and ( $\text{Y}_\text{H}\text{Y}_{\text{HO}_2}$ ) show peak at  $\phi = 1.7$  and thus it is the species H and HO<sub>2</sub> which seem to determine the peak. In order to examine the role of diffusional factors, a calculation of the adiabatic reactor was made and the temperature-time variation for various equivalence ratios is presented in Fig. 15. It can be seen that the fastest heat releasing composition is  $\phi = 1.45$  whereas the fastest flame propagating composition is at  $\phi = 1.7$ . Thus diffusional factors are playing a significant role in causing the shift of the equivalence ratio for peak flame speed from 1.45 to 1.7.

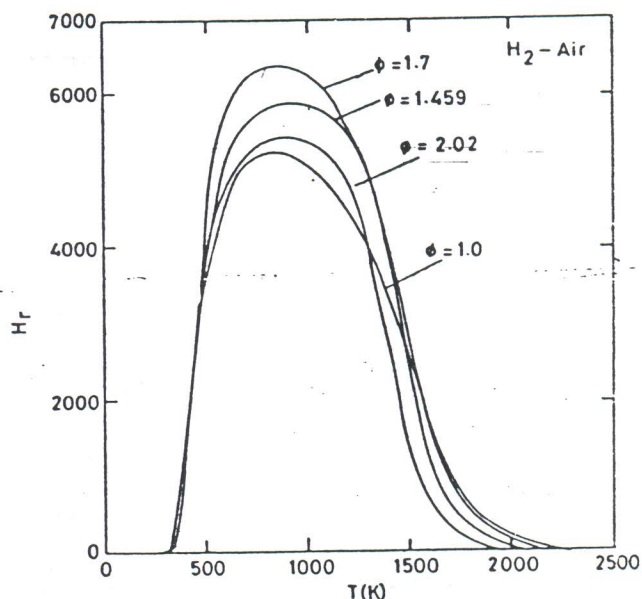


Figure 12: Heat release rates vs Temperature for  $\phi = 1.0, 1.459, 1.7$  and  $2.02$  for H<sub>2</sub>-air

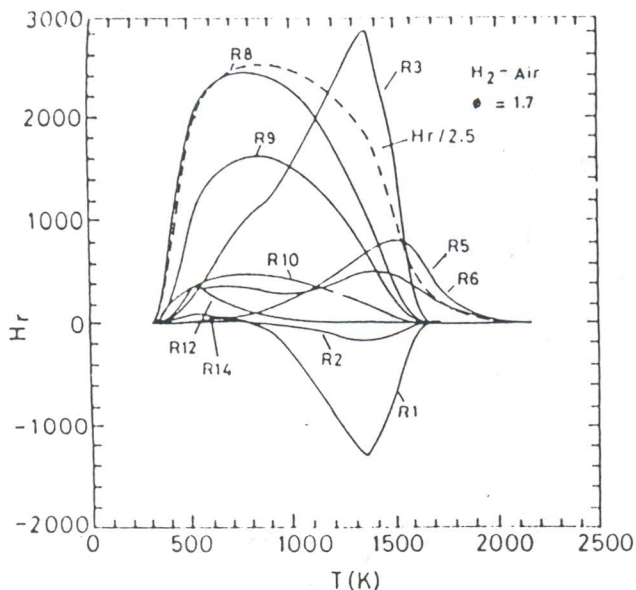


Figure 13: The contribution of various reaction steps to the heat release rates for  $\phi = 1.7$  for  $H_2$ -air system

### Concluding Remarks

In this paper we have discussed two broad features concerning biomass derived fuels: char and producer gas. The reactions of wood char with air/ $CO_2/H_2O$  have shown the relative importances of diffusion and reaction. The reactions with air are diffusion limited, with  $CO_2$  both diffusion and reaction controlled and with  $H_2O$ , larger diffusional control. These are derived from the data of burn time with diameter of the char spheres. It is also shown that vitiated air at 14%  $O_2$  is the limit for extinction of char combustion. All these are predicted through the use of a model based on heterogeneous reactions of char with the reactive gases.

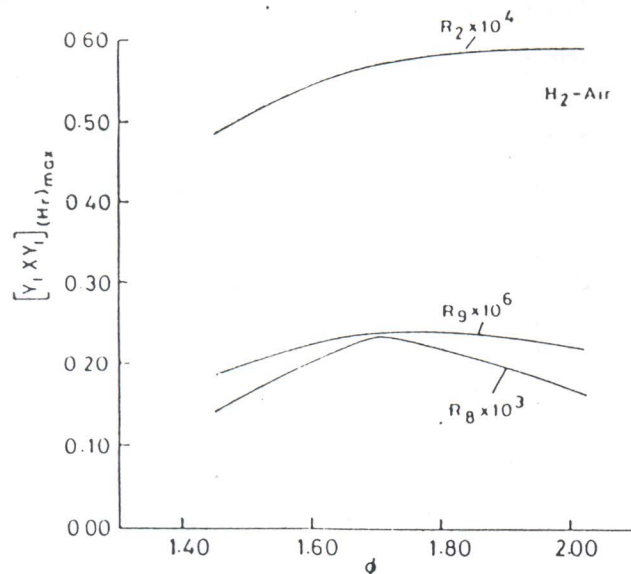


Figure 14: Plot of the product of reactant mass fractions at peak heat release rate with equivalence ratio for  $H_2$ -air systems.

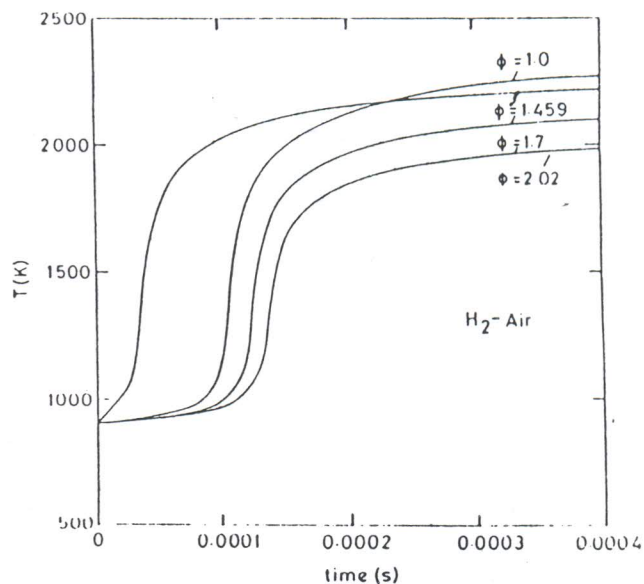


Figure 15: Plot of temperature vs time for an adiabatic reactor ( $H_2$ -air).

The second part of the work is related to the flame speed of producer gas and its components. The plot of heat release rates with non-dimensional temperature is used to draw inferences regarding the importance of chemistry.

The off-stoichiometric peak in flame speed vs mixture ratio behavior found in  $CO$ -air and  $H_2$ -air systems is analysed in terms of the contribution of individual reaction steps to the overall heat release rate. From this, the three or four important reaction steps in which two are common for the two systems are identified. A plot of the product of the mass fraction of the participating species involving the radicals with equivalence ratio is shown to have a peak at the equivalence ratio at which peak in flame speed is observed. It is further shown that chemistry is sufficient to explain the behaviour for  $CO$ -air system and diffusion is also necessary in the case of  $H_2$ -air system.

The issue on which very general conclusions can be drawn concerns the efficacy of the equivalent single step chemistry in combustion theory. It is shown that the ability of equivalent single step chemistry to match the heat release profile is poor for methane-air, carbon monoxide-air and hydrogen-air systems. It is further argued that the poor replication for methane-air system is also seen in the case of other hydrocarbons. Thus it appears that excepting some lean fuel-air systems, a large number of useful fuel-air mixtures may need full chemistry for replication of even the necessary minimum detail, namely the heat release rate profile. A recent study from the laboratory on the extraction of stretch effects on flame speed in premixed gases [32,33] has further substantiated this feature in the case of methane-air, propane-air and hydrogen-air systems.

### References

- [1] Mukunda, H. S., Dasappa, S., and Srinivasa, U. Open-top wood gasifiers. In *Renewable Energy, Sources for fuels and Electricity*, pages 699-728, Island Press, 1993.
- [2] Ergun, S. Kinetics of the reaction of carbon dioxide with carbon. *Jl. Physical Chemistry*, 60:480-485, 1956.
- [3] Dutta, S., Wen, C. Y., and Belt, R. J. Reactivity of coal and char. 1. in carbon dioxide atmosphere. *Ind. Eng. Chem., Process Des. Dev.*, 16 1:20 30, 1977.

